

# Demodulation algorithm for optical fiber fabry-perot interference sensor

Wenhua Wang<sup>1</sup>, Weina Wu<sup>2,\*</sup>, Zhengye Xiong<sup>1</sup>, Wenqing Shi<sup>1</sup>, Yuanzheng Luo<sup>1</sup>, Xiuyun Tian<sup>1</sup> and Zhishan Chen<sup>1</sup>

<sup>1</sup>School of Electronic and Information Engineering, Guangdong Ocean University, Zhanjiang 524088, China

<sup>2</sup>School of mathematics and computer, Guangdong Ocean University, Zhanjiang 524088, China

**Abstract.** In view of resolution of optical fiber Fabry-Perot (FP) interference sensor, this paper analyses and researches high resolution demodulation algorithms including fast Fourier transform demodulation algorithm, cross-correlation calculation demodulation algorithm, vernier demodulation algorithm. Through continuous improvement, the vernier demodulation algorithm has achieved a resolution of 0.084nm. And it has a resolution of 2.3Pa when the vernier demodulation algorithm was applied to osmotic pressure measurement.

## 1 Introduction

Optical fiber sensors are widely used in the fields of industry, national defence, medical treatment and scientific research [1, 2]. Optical fiber Fabry-Perot interference (OFFPI) sensor as one important sensor can be divided into two categories: intrinsic type and extrinsic type. After their successful production in 1988 [3] and 1991 [4] respectively, investigators have done substantial research on the sensor's structure, materials, preparation technology, and demodulation algorithm [5-19]. And also, extrinsic OFFPI sensors are divided into diaphragm-free type [5-8] and diaphragm type [13-18]. Various demodulation algorithms are then constantly proposed in view of resolution of sensors [20-23]. By demodulation of the interference spectrum signal, variation of cavity length can be calculated, and variation information of the parameter to be measured can be reversed. Therefore, demodulation algorithm is very important for sensor performance improvement. In this paper, we analysed and researched the various demodulation algorithms. The experimental results of some practical applications indicate that the algorithms have good performance.

---

\* Corresponding author: [wuwn@gdou.edu.cn](mailto:wuwn@gdou.edu.cn)

## 2 Demodulation algorithm

### 1.1 Fast Fourier transform (FFT) demodulation algorithm

The interference spectrum accessed from the wavelength detector such as Si720 (Micro Optics Inc.) is a wavelength domain signal. For signal processing means of FFT, the spectrum signal should be transformed to frequency domain according to the relationship of  $f=c/\lambda$ . After filtering the DC component, the optical frequency domain can be expressed as :

$$I(f) = 2RI_0 \cos\left(\frac{4\pi Lf}{c} + \pi\right) \tag{1}$$

where, L is the length of FP cavity. To facilitate computer processing of discrete finite-length data sequence, discrete Fourier transform is adopted. The discrete Fourier transform of the finite-length data sequence  $x(n)$  is expressed as :

$$X(k) = \sum_{n=0}^{N-1} x(n) \exp\left(-j\frac{2\pi}{N}nk\right), \quad k = 0, 1, \dots, N-1 \tag{2}$$

where, N is the data sequence length, that is, the number of sampling points. After discrete Fourier transform, assume that the optical frequency interval is  $\Delta f$ , then the  $\Delta f$  is:

$$\Delta f = \frac{c}{\lambda} - \frac{c}{\lambda + \Delta\lambda} = \frac{c\Delta\lambda}{\lambda(\lambda + \Delta\lambda)}, \quad \text{where, } \Delta\lambda = \frac{\lambda_2 - \lambda_1}{N} \tag{3}$$

It can be seen from the above formula that the optical frequency interval gradually decreases as the wavelength increases, which is uneven, while the independent variables involved in FFT operation must be equally spaced. Therefore, it is necessary to interpolate the frequency domain spectral signal to access the sampling signals at equal frequency intervals. Otherwise, the cavity length calculated by FFT will have a deviation, leading to lower resolution. PhD Zhou Xinlei demodulates the spectral signal using cubic spline interpolation and Gaussian interpolation [23], and the resolution has increased by one time, reaching to 7nm, as shown Fig. 1.

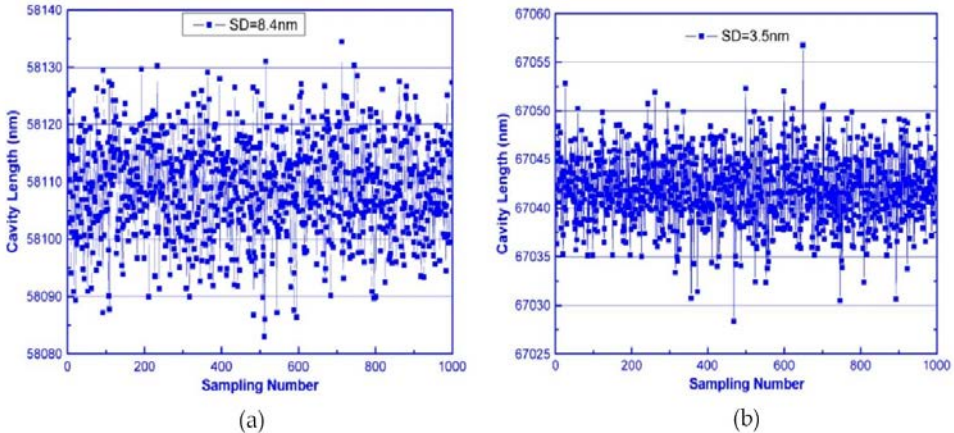


**Fig. 1.** Resolution of the FFT demodulation algorithm (a) before and (b) after processing with the cubic spline interpolation and Gaussian interpolation.

## 1.2 Cross-correlation calculation demodulation algorithm

The cross-correlation calculation demodulation algorithm is a high-resolution demodulation algorithm proposed by research group of prof. Yu Qingxu [20]. In terms of wavelength domain, OFFPI sensor has an unknown cavity length  $L_0$  and the normalized spectrum of the real output interference spectrum  $L_1 < L_0 < L_2$  after filtering of DC component can be expressed as :

$$I_{nl}(\lambda) = 2 \cos\left(\frac{4\pi L_0}{\lambda} + \pi\right) \tag{4}$$

Then construct a virtual normalized interference signal and perform correlation operation with the formula (4). Set its cavity length to  $L$  and interference contrast to 1, then

$$I_{nv}(\lambda) = 2 \cos\left(\frac{4\pi L}{\lambda} + \pi\right), \quad L_1 < L < L_2 \tag{5}$$

Hence, the correlation function of equation (4) and equation (5) is :

$$C(L) = \int_{\lambda_1}^{\lambda_2} I_{nl}(\lambda) I_{nv}(\lambda) d\lambda = 4 \int_{\lambda_1}^{\lambda_2} \cos\left(\frac{4\pi L_0}{\lambda} + \pi\right) \cos\left(\frac{4\pi L}{\lambda} + \pi\right) d\lambda, \quad L_1 < L < L_2 \tag{6}$$

When cavity length of the virtual FP cavity is equal to the actual cavity length, the cross-correlation function coefficient  $C(L)$  reaches the maximum. Therefore, FP cavity length can be accurately derived from the acquired real interference signal. Its discrete form is :

$$C(L_m) = \Delta\lambda \sum_{i=1}^N x(n) \cos\left(\frac{4\pi L_m}{\lambda_n} + \pi\right) \tag{7}$$

where,  $\Delta\lambda$  is the wavelength sampling interval when discretizing at equal intervals,  $L_m$  is the cavity length sequence when discretizing at equal intervals,  $x(n)$  is the spectral intensity data sequence accessed by the detector, and  $\lambda_n$  is the corresponding wavelength of  $x(n)$  element,  $N$  is the total number of spectral signal intensity data series.

## 2.3 Minimum Mean Square Error Estimation Demodulation Algorithm

The minimum mean square error estimation algorithm was first proposed by research group of prof. Yu Qingxu [23]. The algorithm evaluates the measured cavity length of extrinsic OFFPI sensor using mean square error, which is related to the parameter estimation theory. The mean square error is defined as the expectation of the square of difference between the estimator and its true value, which can be expressed as :

$$MSE = E\left\{(\bar{\theta} - \theta)^2\right\} = E\left\{\left[\bar{\theta} - E(\bar{\theta})\right]^2\right\} + \left[E(\bar{\theta}) - \theta\right]^2 \tag{8}$$

where, the first term on the right side of the second line of the equation is the variance of the estimator, which represents the expected value of the square of difference between the estimator  $\bar{\theta}$  and its expected value  $E(\bar{\theta})$ , and its size represents the degree of dispersion between the estimator  $\bar{\theta}$  and its expected value  $E(\bar{\theta})$ . Hence, a smaller variance indicates

that estimator is more concentrated near its expected value. The second term is the square of the estimator's deviation which represents the difference between the estimator's expected value  $E(\bar{\theta})$  and its true value  $\theta$ . Therefore, a smaller deviation indicates that the estimator is closer to the true value of the parameter. We believe that the estimator with minimum mean square error is more effective. At this time, the estimator with small deviation and dispersion is concentrated near the expected value. Therefore, the mean square error is an effective means to evaluate the best estimate.

The information derived from the sensor is the interference spectrum signal with the actual cavity length  $L_0$ , which is normalized and discretized into a spectrum sequence, and each element is indicated by  $x(n, L_0)$ . The ideal interference spectrum signal also adopts the same discrete processing method, and the elements in the discrete spectrum sequence can be expressed as :

$$I(n, L) = 2R(1 + \cos(\frac{4\pi L}{\lambda_0 + n \cdot \Delta\lambda} + \pi)) \tag{9}$$

Therefore, the mean square error between the best estimate  $L$  and the true value  $L_0$  of FP cavity length can be expressed as :

$$MSE(L) = \frac{1}{N} \sum_{n=0}^{N-1} (x(n, L_0) - I(n, L))^2 \tag{10}$$

where,  $N$  is the total number of discrete data sequence elements.

### 2.4 Vernier demodulation algorithm

Based on the research team results, in view of the problem that the minimum mean square error estimation demodulation algorithm may have "mode jump" when increasing the dynamic range, Zhou Xinlei proposed a vernier demodulation algorithm based on FFT and minimum mean square error estimation [23]. FFT is used to pre-position the FP cavity length, and then this pre-position is taken as the reference of the mean square error estimation range. The estimation range is determined according to the actual demodulation speed within the longitudinal mode interval, thereby further optimizing the demodulation algorithm of FP cavity length without "mode jump" problem. Therefore, vernier demodulation algorithm combines the characteristics of FFT and the minimum mean square error estimation demodulation algorithm to achieve high-resolution spectral signal demodulation in large dynamic range while addressing "mode jump" problem and removing the contradiction that the demodulation dynamic range and resolution cannot be solved at the same time.

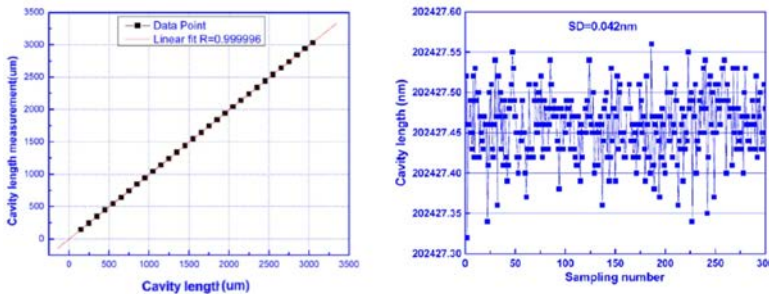


**Fig. 2.** Experimental results of the (a) measurement range and (b) measurement SD.

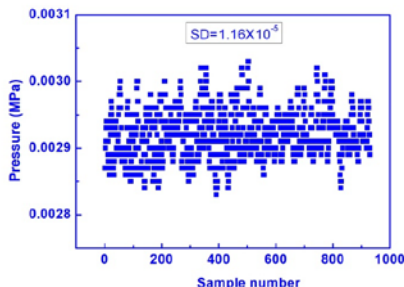


**Fig. 3.** Measurement SD of OFFPI osmotic pressure sensor.

### 3 Results of vernier demodulation algorithm

In order to verify experimentally the performance of the vernier demodulation algorithm, the OFFPI sensor is applied to displacement measurement under a large dynamic range of 3mm, as shown in Fig. 2. Fig. 2 (a) shows the results of the cavity length demodulation, and Figure 2 (b) shows the experimental results of the resolution measurement, in which the standard deviation (SD) is 0.042 nm. If twice as much as the SD is taken as the resolution of the sensor, then the demodulation resolution of the sensor based on the vernier demodulation algorithm is 0.084 nm.

And also, vernier demodulation algorithm is also applied to signal demodulation of OFFPI osmometer. After demodulation, the cavity length change of the sensor within 15 minutes is shown in Fig. 3. The standard pressure deviation of the sensor at 0MPa is  $1.16 \times 10^{-2}$  kPa, which is doubled as the sensor resolution, then the sensor pressure resolution is about 2.3Pa.

### 4 Conclusions

The signal demodulation method relates to the level of performance parameters such as the resolution and measurement accuracy of OFFPI sensor. This paper discusses the commonly used demodulation algorithms and the high-resolution demodulation algorithm of OFFPI sensor. Through continuous improvement, the vernier demodulation algorithm has achieved a resolution of 0.084nm and good potential application in the osmotic pressure field.

This research was funded by the Naural Science Foundation of Guangdong Province (2019A1515010835), Characteristic Innovation Project of Guangdong Universities (2019KTSCX054), the Science and Technology Planning of Guangdong Province (2015A030401094), and the Scientific Research Startup Foundation of Guangdong Ocean University (R19028), China.

### References

1. Y. Wang, Y. Yuan, X. Liu, Q. Bai, H. Zhang, Y. Gao, B. Jin, IEEE Access **7**, 85821 (2019)
2. A.R. Camilo, Díaz, L. Arnaldo, M. Carlos, F. Anselmo, J.P. Maria, IEEE Sens. J. **19**, 7179 (2019)
3. C. Lee, H.F. Taylor, Electron. Lett. **24**, 193 (1988)
4. A.M. Kent, F.G. Michael, M.V. Ashish, O.C. Richard, Opt. Lett. **16**, 273 (1991)
5. S.H. Aref, H. Latifi, M.I. Zibaii, M. Afshari, Opt. Commun. **269**, 322 (2007)

6. G. Zhang, M. Yang, M. Wang, Opt. Fiber Technol. **19**, 618 (2013)
7. G. Beheim, K. Fritsch, R.N. Poorman Rev. Sci. Instrum. **58**, 1655 (1987)
8. R.A. Wolthuis, G.L. Mitchell, E. Saaski, J.C. Hartl, M.A. Afromowitz, IEEE Trans. Biomed. Eng. **38**, 974 (1991)
9. J. Li, Z. Li, J. Yang, Y. Zhang, C. Ren, Opt. Laser Technol. **129**, 106296 (2020)
10. K. Tian, M. Zhang, J. Yu, Y. Jiang, H. Zhao, X. Wang, D. Liu, G. Jin, E. Lewis, G. Farrell, P. Wang, Sens. Actuator A-Phys. **310**, 112048 (2020)
11. Y. Zhu, M. Han, Opt. Lett. **45**, 34192 (2020)
12. J. Tian, Q. Zhang, T. Fink, H. Li, W. Peng, M. Han, Opt. Lett. **37**, 4672 (2012)
13. J. Eom, C. Park, B. Lee, J. Lee, Sens. Actuator A-Phys. **225**, 25 (2015)
14. J. Shi, Y. Wang, D. Xu, IEEE Photonics J. **5**, 1 (2016)
15. C. Zhu, Y. Chen, Y. Zhuang, G. Fang, X. Liu, J. Huang, IEEE Trans. Instrum. Meas. **67**, 950 (2018)
16. J. Zhu, M. Wang, L. Chen, Opt. Fiber Technol. **34**, 42 (2017)
17. Z. Gong, K. Chen, X. Zhou, J. Lightwave Technol. **35**, 5276 (2017)
18. C. Li, X. Yu, T. Lan, J. Liu, S. Fan, IEEE Photonics Technol. Lett. **30**, 565 (2018)
19. X. Zhou, Q. Yu, W. Peng, Opt. Lasers Eng. **121**, 289 (2019)
20. K. Chen, Z. Wang, M. Guo, B. Liu, Q. Yu, Opt. Eng. **58**, 026106 (2019)
21. L. Liu, S. Wang, W. Ni, X. Fu, D. Liu, J. Zhang, IEEE Photonics J. **9**, 16795170 (2017)
22. Z. Yu, A. Wang, IEEE Photonics Technol. Lett. **27**, 817 (2015)
23. X. Zhou, Q. Yu, IEEE Sens. J. **11**, 1603 (2012)